Coupled Sensory Interneurons Mediate Escape Neural Circuit Processing in an Aquatic Annelid Worm, *Lumbriculus variegatus*

Zane R. Lybrand[1], Veronica G. Martinez-Acosta[2] and Mark J. Zoran[3*]

[1]Department of Biology, University of Texas, San Antonio, TX

[2]Department of Biology, University of the Incarnate Word, San Antonio, TX

[3]Department of Biology, Texas A&M University, College Station, TX

*Corresponding Author: Dr. Mark J. Zoran, Department of Biology, Texas A&M University College Station, TX 77843-3258; Phone# (979) 845-8099; email: mjzoran@tamu.edu

Running Title: Annelid sensory processing interneurons

Manuscript: 30 pages, 8 figures, 2 tables

Words in (i) manuscript (5,928), (ii) abstract (170), (iii) introduction (448), (iv) discussion (1,609)

This article has been accepted for publication and undergone full peer review but has not been through the copyediting, typesetting, pagination and proofreading process which may lead to differences between this version and the Version of Record. Please cite this article as doi: 10.1002/cne.24769

Acknowledgments

We would like to thank Rick Littleton and the staff of the TAMU Microscopy & Imaging Center. Also, we thank Dr. Joseph Szule, Dr. Mark Harlow, Robert Marshall and Dr. Jack McMahan for their aid and advice on the ultrastructure of synapses. We also thank Chace Craig for help with experiments along with a number of undergraduate researchers: Yuan Xing, Stephanie Oliver, Megan Florez, and Natalie Nagy.

Data Availability Statement

The data that support the findings of this study are available from the corresponding author upon reasonable request.

Abstract

The interneurons associated with rapid escape circuits are adapted for fast pathway activation and rapid conduction. An essential aspect of fast activation is the processing of sensory information with limited delays. Although aquatic annelid worms have some of the fastest escape responses in nature, the sensory networks that mediate their escape behavior are not well defined. Here, we demonstrate that the escape circuit of the mud worm, *Lumbriculus variegatus*, is a segmentally-arranged network of sensory interneurons electrically coupled to the central medial giant fiber (MGF), the command-like interneuron for head withdrawal. Electrical stimulation of the body wall evoked fast, short-duration spikelets in the MGF, which we suggest are the product

of intermediate giant fiber (IGF) activation coupled to MGF collateral dendrites. Since these contact sites have immunoreactivity with a glutamate receptor antibody, and the glutamate receptor antagonist CNQX abolishes evoked MGF responses, we conclude that the afferent pathway for MGF-mediated escape is glutamatergic. This electrically-coupled sensory network may facilitates rapid escape activation by enhancing the amplitude of giant axon depolarization.

KEYWORDS

annelid, couple network, electrical synapse, giant interneuron, sensory processing, silent synapse, RRID:AB_1566261, RRID:AB_880229, RRID:AB_396353, RRID:AB_141596, RRID:AB_1500929, RRID:AB_141357

INTRODUCTION

Neural circuits for rapid escape exist in a wide range of animals, including annelids, arthropods, mollusks and vertebrates. Some common structural features that promote behavioral speed are present within these diverse escape networks, including axonal gigantism (Hartline and Colman, 2007), glial-derived myelination (Schweigreiter et al., 2006), and electrical synaptic connectivity (Pereda, 2014). The central interneurons associated with these pathways typically possess large axons, or giant fibers (GFs) for fast conduction. Although escape systems are often called reflexive, it is now clear that they are much more flexible and require computational decisions based on sensory inputs, often presented in the midst of other conflicting cues (Herberholz and Marquart, 2012). Although escape reflexes of annelid worms have been long studied (Drewes, 1984), their underlying sensory networks are not well understood, particularly how environmental stimuli are quickly processed to rapid withdrawal behavior.

In annelid earthworms, rapid escape shortening is initiated by mechanical sensations, where stimuli detected by anterior segments of the animal's body activate a medial giant fiber (MGF) interneuron pathway and head withdrawal, whereas stimulation of posterior segments activates a lateral giant fiber (LGF) interneuron pathway and tail withdrawal (Drewes, 1984). These GF pathways and the behaviors they mediate are highly conserved, yet the habitats these animals occupy and the cues that trigger their escape are quite diverse (Zoran and Drewes, 1987). Little is known about the sensory networks within the ventral nerve cord (VNC) that mediate escape in oligochaete worms, other than they involve mechanosensory neuron inputs

(Smith and Mittenthal, 1980) that trigger giant interneuron activation. A major impetus for this study was to elucidate the sensory processing pathway employed by the aquatic oligochaete worm, *Lumbriculus variegatus*, for activation of its MGF-mediated escape.

The sensory processes involved in the escape circuit of *Lumbriculus* are highly plastic. For example, sensory fields rapidly transform following body fragmentation (Drewes and Fourtner, 1990; Martinez et al., 2005). MGF sensory inputs and MGF-mediated escape responses emerge within 6-24h in segments that previously had neither (Lybrand and Zoran, 2012). To understand the nature of lumbriculid worm sensory processing, we have investigated the structure and function of the MGF interneuronal pathway. Our findings reveal a network of interneurons electrically coupled to the MGF. Structural reconstructions of the coupled network, combined with electrophysiological and immunocytochemical staining, indicate that the electrically coupled synapses are associated with intermediate sensory interneurons that themselves receive glutamatergic chemical inputs from sensory neurons. Thus, these sensory circuits converge like multiple spokes of a wheel upon MGF collateral dendrites that function as a central hub for information processing. These sites of sensory convergence might be ideal for synchrony, summation and facilitation of sensory synaptic inputs and, consequently, the activation of the escape central commands.

MATERIALS AND METHODS

Animal cultures

Lumbriculus variegatus cultures were purchased from Flinn Scientific (Batavia, IL) and housed in bins filled with aerated fresh water at a temperature of 16ºC. Brown paper towels were cut into one-inch squares and used as substrate material. The worms were fed a weekly diet of powdered Algae-Feast™ *Spirulina* (Aquatic Eco-Systems Inc., Apoka, FL). For dissections, worms were immobilized in a 0.25 µM nicotine (Sigma, St. Louis, MO) and spring water (Ozarka, Oklahoma City, OK). Exposure of this annelid worm to nicotine causes reversible paralysis without subsequent inpacts on reproduction, regeneration (Martinez et al., 2005) or synaptic physiology (Lybrand and Zoran, 2012). Dissection involved anterior-posterior incision and exposure of the nerve cord by removal of the gut.

Electrophysiology and pharmacology

Current clamp recordings were performed on reduced preparations of *Lumbriculus variegatus.* These preparations consisted of body segments opened with a dorsal incision and pinned to a silicone dish. Following removal of gut tissue, the preparation was treated for 5 minutes with worm saline (75mM NaCl, 4mM KCl, 2mM CaCl, 2mM MgCl, 10mM Tris, 23 mM sucrose). (Zoran et al., 1988), 25µM 6-Cyano-7-nitroquinoxaline-2,3-dion (CNQX; Sigma-Aldrich) in a <0.1% DMSO saline solution, or 100µM D-2-Amino-5-phosphonophentanoic acid (AP5; Sigma-Aldrich) in worm saline. At the end of the 5-minute treatment, a one-minute

electrophysiological recording was performed. MGF microelectrode penetrations were difficult to maintain and, therefore, sustained resting membrane potential recordings during media exchange were not feasible. Rather, microelectrode recordings were made from medial giant axons within neighboring body segments (i.e., interneurons from different nerve cord segments) for each drug group. For washout data, separate preparations were treated for the 6 minutes with drugs and the treatment solution was then replaced with worm saline for an additional 5 minutes before the washout recordings were performed. These protocols were developed to avoid multiple penetration of any single giant interneuronal axon and the variability that would impose.

Spontaneous and evoked post synaptic potentials (PSP) were recorded from anterior segments within the medial giant fiber sensory field using procedures previously described (Lybrand and Zoran, 2012). For sensory activation, an electrical stimulus (0.2 ms duration) was applied to the body wall with a suction electrode, using a Stimulus Isolation Unit (direct coupled mode; Grass, West Warwick, RI) with increasing voltage amplitude (2–5 V) until 100% of all stimuli activated postsynaptic potentials in the MGF. Body wall segments were stimulated with 20–30 pulse at low frequency (0.2 Hz) within a given segment. These parameters were used in all subsequent recordings to activate sensory inputs. The MGF was penetrated with a borosilicate glass microelectrode (tip resistance of 10-25 MΩ) filled with 1.5 M KCl pipet solution. Amplitudes of evoked PSPs were measured using Clampfit 10.0 software (Molecular Devices, Sunnyvale, CA). A semi-automated event-detection protocol within Clampfit 10.0 was used to analyze spontaneous events. A template waveform was generated

from >100 events recorded from the MGF in anterior worm segments and was used for event detection. In pharmacology experiments, stable resting membrane potentials (-60mV) were maintained in reduced preparations and then synaptic physiology was assessed for one minute.

Dye Injections

For giant fiber injections, worms were immobilized in nicotine, dissected and pinned to silicone dishes as described above. MGF axons were injected using micropipettes filled with a saline solution (75mM NaCl, 4mM KCl, 2mM CaCl, 2mM MgCl, 10mM Tris, 23 mM sucrose) containing lucifer yellow (3%; Sigma), fast green (saturated; Sigma), and rhodamine dextran (3%; Molecular Probes) or Neurobiotin (1:1000; Vector Laboratories, Burlingame, CA) using a picospritzer **(**General Valve). Once injected, preparations were incubated in worm saline for 30 minutes at room temperature to allow dye diffusion. For Neurobiotin fills, injected fragments were incubated in Fluorescein Avidin D (1:1000; Vector Labs) in phosphate buffered saline (PBS) overnight at 4ºC, followed by an extensive PBTD (PBS + 0.1% DMSO + 0.1% Tween ®20; Sigma Aldrich) wash, and a secondary incubation in anti-avidin conjugated to fluorescein (1:1000; Vector Labs) overnight at 4ºC. Prior to imaging, fragments were dehydrated with a series of five ethanol baths (70%, 80%, 95%, 95%, and 100% EtOH) at 10 min each and were cleared by emersion in methyl salicylate prior to being mounted on glass slides.

Antibody characterization

A number of glutamate receptor antibodies were used to identify the location of glutamate receptors in the ventral nerve cord of *Lumbriculus variegatus* (Table 1). The monoclonal antibody GluR5,6,7 (RRID: AB_1566261) recognizes the GluR5, GluR6, and GluR7 subunits of AMPA/kainate receptors. The GluR5 N-terminal extracellular domain was used as the immunogen and was shown not to recognize GluR1,2,3, or 4 AMPA/kainate receptors (Huntley et al., 1993). The GluR 5-7 was described to be made against a sequence of extracellular domain of the GlurR 5 receptor subunit (aa: 233-518) and recognizes kainite receptor subtypes GluR 5, GlurR 6, and GlurR 7 subunits (Huntley et al., 1993). GluR5-7 immunoreactivity has also previously been identified throughout the neuropile of another annelid, the leech *Hirudo* (Thorogood et al., 1999). The GluR2,3 antibody (RRID: AB_880229) was characterized by the manufacturer (Table 1) and was specific to both phosphorylated and unphosphorylated GluR2,3 subunits on the Serine 880/891 of mature human brain tissue. A polyclonal GluR2,3 antiserum against a C-terminal domain (aa: 850-862) of AMPA receptor subtype was also reactive in leech (Thorogood et al., 1999). Antibodies against the N-Methyl-D-Asparate Receptor-1 (NR1; RRID: AB_396353) were previously generated from the extracellular loop between transmembrane domains 3 and 4 (clone 54.1) (Siegel et al., 1995). In leech whole mount preparations, no NR1 immunoreactivity of microglia was detected (Thorogood, 1999). However, western blot analysis of leech nerve cord, using the same antibody, identified a protein similar in size (Grey et al., 2009). Preparation and preadsorption of mouse anti-GluR5-7 in monkey brain showed an absence of the GluR5 subtype staining (Huntley

et al., 1993). Preadsorption controls of mouse anti-GluR2,3 and anti-NR1 in rat brain resulted in in absence of staining (Petralia and Wenthold, 1992; Petralia et al., 1994).

Secondary antibodies conjugated to fluorescent markers were used for all primary antibodies (Table 2). For all experiments, parallel negative controls were processed along with all preparations. To do this, sections were incubated with secondary antibody only and no positive immunofluorescence was detected. Isotype controls were also run for each antibody. Secondary antibodies from the same species but different isotype (IgG or IgM) were incubated with the primary antibody to determine tissue specificity and background levels.

Immunohistochemistry and imaging

Worms were immobilized in 0.25µM nicotine in spring water, pinned on a silicone dish, and fixed with a 4% paraformaldehyde solution for 30 minutes at room temperature. Fixed preparations were washed in PBS. Fragments were placed in a 30% sucrose solution for 12 hours before being embedded in Tissue Freezing Medium (TFM™; Triangle Biological Solutions, Durham, NC) and were frozen at -80°C. Blocks were cut using a cryostat (Leica) and cross-sections were mounted on Colormark™ Plus slides (Erie Scientific Company, Portsmouth, NH) and dried overnight. Dried slides were washed with PBTD for 30 minutes before blocking for 2h in a solution of PBS and 5% fetal goat serum was applied. Sections were treated with primary antibodies diluted in blocking serum overnight at 4°C. Primary antibodies used were GluR5-7

(1:50; Abcam), GluR2, 3 (1:33; Abcam), and NR1(1:33; BD Pharmingen) (Table 1). After wash with PBTD, sections were treated with fluorescent secondary antibodies, Alexa Fluor® 488 goat anti-mouse IgM, Alexa Fluor® 488 goat anti-rabbit IgG, and Alexa Fluor® 568 goat anti-mouse IgG (1:1000; Invitrogen). DAPI (4',6-Diamidino-2-Phenylindole, Dihydrochloride) was included in the secondary incubation for nuclear staining in all preparations (1:1000; Invitrogen). Slides were then washed and ProLong® Gold Antifade reagent (Invitrogen) was added. Imaging was done on an Olympus IX70 inverted microscope and CoolSnapHQ camera (Actimetrics, Wilmette, IL). Fluorescent intensity was measured by selecting regions of interest (ROI) using Simple PCI6.0 imaging software (Compix, Inc., Cranberry Township, PA). For each image, four ROI around each giant fiber, four randomly selected neuropile and four background values were measured. An average value for LGF, MGF, VGF, neuropile and background were calculated and statistically analyzed with the same ROI values from all other images. For all fluorescent intensity data presented, the average background intensity was subtracted from all average ROI values.

Electron microscopy

Anterior and posterior fragments from non-regenerating worms were fixed by immobilizing in 25μM nicotine solution and immersed in 3% glutaraldehyde/worm saline (500 mOsM total) overnight. Anterior fragments consisted of 6-10 segments from the first quarter of the worm and posterior fragments were 30 segments from the posterior quarter. Fragments were

then washed hourly in worm saline for 5 hours and post fixed in 2% osmium tetroxide and worm saline for 2 hours. Following post fixation, fragments were rinsed in 33mM PBS for 30 minutes and washed 20 minutes in deionized water. Fixative and buffer solutions were maintained at ±4°C with a pH around 7.2 (Kensler et al., 1979). Fragments were dehydrated in an acetone series (10, 20, 30…90, 95, 100, 100, and 100%) on ice with care to prevent exposure to air and stored at 0°C overnight.

Prior to embedding, fixed fragments were transferred into propylene oxide. In order to ensure proper infiltration of plastic resin, fragments were placed in increasing percentages of Epon-Araldite mixture over 24 hours. Samples were then flat embedded in a small aluminum dish with fresh Epon-Araldite and baked at 60°C for 48 hours. Ultra-thin sections (about 70nm) from anterior and posterior blocks were stained with uranyl acetate in methanol and aqueous lead citrate. Conventional transmission electron microscopy with JOEL1200 EX equipped with a 3kx3k SIA lens-coupled CCD slow-scan camera was used to examine sections.

Statistics

Statistical significance was analyzed using a Mann-Whitney test for non-parametric data (Excel 2010, Microsoft) and presented as p-values where indicated $p<0.05$ considered significant. Variation was presented as standard deviation. All statistics were performed using GraphPad with Prism8, following its Statistics Guide.

RESULTS

Medial giant fiber (MGF) coupled network

Synaptic inputs to, and outputs from, the myelinated giant axons of oligochaete worms are thought to be located at unmyelinated collaterals that project ventrally into the neuropile of the nerve cord (Drewes, 1984; Zoran et al., 1988). In order to visualize the interneuron collaterals of *Lumbriculus* medial giant fibers (MGF), the fluorescent dye Lucifer yellow (LYCH; 450 Da) was injected into the MGF axons of anterior (n=6 preparations) or posterior (n=3 preparations) body segments. LYCH diffused along several (~4-5) segments of medial giant axon, passing across the septal boundaries between neighboring axons in both anterior and posterior directions. Septal boundaries (SB) were identifiable as chevron-shaped aggregations of dye where the axonal membranes are apposed (Figure 1a) and gap junction plaques exist (Gunther, 1975). A larger molecular weight dye, rhodamine dextran (10 KDa), did not diffuse across septal boundaries (data not shown). LYCH also accumulated at medial collateral (MC) projections spaced at approximately 100 µm intervals along the giant axon (Figure 1a). MC projections are small protrusions through the myelin-like sheath that surrounds the giant fibers to form an unmyeinated dendritic hub for synaptic integration within the neuropile. Efferent connections from the VNC, for example motor neurons, are thought to form synapses along MC projections in each segment. In addition to approximately 4 medial collaterals per segment, a single axonal branch extended to the medial soma (MS) in each body segment, confirming the segmental origin of this multicellular fiber pathway in *Lumbriculus* (Figure 1a and 2a). No

differences in gross MGF structure, as revealed by LYCH, were observed between anterior and posterior segments.

LYCH injections revealed strong dye diffusion among the segmentally arranged medial giant interneurons, but no dye was observed with other neurons of the VNC, suggesting strong gap junctional coupling between medial giant interneurons (Figures. 1a and 2a). To better investigate potential coupling of the MGF with sensory or motor neurons, neurobiotin (NB; 320 Da), a dye of opposite charge and lower molecular weight was injected into the MGF of anterior (n=20 preparations) or posterior (n=8 preparations) body segments. In contrast to LYCH injections, multiple neuronal cell bodies and axonal tracts were labeled within the VNC (Figure 1b), but again no neuronal processes exited the VNC and no neurobiotin was detected in motor neurons. Besides the MS, four laterally located cell bodies and four medially located cell bodies were dye-coupled to the MGF in each body segment (Figure 1b). Two small intermediate giant fibers (IGF) were dye coupled to the medial giant interneuron, with each extending parallel to the dye-filled MGF along the VNC (Figure 1c). The IGFs were much smaller in diameter than the MGF and were located ventrolaterally within the neuropile and appeared connected by multiple fine cross-bridges within each segment (Figure 1c). A consensus structure of the MGF coupled network in longitudinal perspective was created based upon 37 dye-fill preparations (Figure 1d), where the coupled network is operationally defined as the set of cells labeled following injection of tracer into the MGF. The network consists of nine interneurons per segment coupled to three giant axons, including the MGF and two smaller IGFs. The septal boundaries (SB) of the giant

axons are located mid segment along with four IGF crossbridges (CB) and four medial collaterals (MC), one of each closely associated at four equally spaced positions along the VNC. This neural anatomy appears similar across both anterior and posterior segments.

The medial giant axon has a diameter of 20-40 μm and its soma is located in the ventral part of the nerve cord. The medial cell body is connected to the giant axon by an axonal branch emerging from the MGF several hundred micrometers from the inter-axon septal boundary (Figure 2a). The intermediate giant axons have diameters of 2-4 μm and their somata are positioned laterally within the VNC and connect to the IGFs by fine processes (Figure 1b and c). The branch medial collaterals are large, globular bouton-like structures that terminate in the neuropile ventral to the medial giant axon (Figure 2a). Serial cross-sections of NB-filled preparations confirmed coupling of the MGF the bilateral IGFs (Figure 2c). Thus, a consensus structure of the MGF coupled network in cross-section based on 6 preparations illustrates the relationship between cell bodies to giant fiber pathways (Figure 2d). Since no LYCH- or NB-filled processes were detected outside of the VNC, this interneuronal network is not electrically coupled to sensory or motor processes that project from or to peripheral targets.

Ultrastructure of the MGF coupled network

Sensory inputs to MGF collaterals of oligochaete worms appear to be indirect, involving interposed interneurons thought to function as afferent processing relays (Drewes, 1984). We conducted transmission electron microscopy (TEM) of MGF pathways and followed their

collaterals and IGF crossbridges through serial sections. Similar to collateral architecture identified in other oligochaete worms (Jamieson, 1981; Zoran et al., 1988), MGF collaterals protrude through the myelin-like sheathing of the giant axon (Figure 3a). Collaterals of the MGF in both anterior and posterior body segments contained clusters of small translucent synaptic vesicles, which were localized to the lateral edges of the protruding processes (Figure 3b). These synaptic vesicle clusters likely represent interneuronal synaptic outputs to escape motor neuronal pathways (Drewes, 1984). No evidence of chemical synapses onto the medial collaterals was found, suggesting that if not absent, such chemical inputs at collaterals are rarer than outputs.

The IGFs are located in bundles of 4-5 small diameter (1-4 μm) unmyelinated axons within the VNC neuropile (Figure 3c). Extensive chemical synaptic contacts were observed terminating onto the IGFs and associated fibers of the interneuronal bundle (Figure 3d). These synaptic terminals were associated with plasma membrane thickenings, reminiscent of pre- and postsynaptic densities, and contained predominately small translucent vesicles, along with some dense core vesicles. IGF bundles were continuous with axonal cross-bridges that projected medially and closely apposed MGF collateral membranes (Figure 3a-c). Therefore, synaptic inputs onto the IGF bundles might constitute an indirect pathway, via their crossbridges, for sensory processing and activation of the MGF pathway.

In order for IGF bundles to deliver interneuronal synapse signals to the MGF pathways, sites of contact between these two giant fiber systems much exist. TEM of cross-sections through the nerve cord were examined in search of such IGF-MGF contacts (Figure 4a). Within the VNC

neuropile, IGF crossbridges terminated in direct apposition to MGF collateral (MC) membranes (Figure 4b-c). High magnification of sites of collateral-crossbridge contact revealed no evidence of chemical synaptic ultrastructure.

Electrophysiology of the MGF coupled network

Two types of action potentials, small and large amplitude, are recorded intracellularly from MGF axons (Lybrand and Zoran, 2012), when electrical stimulation is delivered to body segments of a dissected worm (Figure 5a). Body wall stimulation elicits subthreshold excitatory postsynaptic potentials (EPSPs) in the MGF, which when of sufficient threshold amplitude triggered both MGF action potentials (Figure 5b) and small spikelets (Figure 5c and d). Both large and small spikes are all-or-none, with spikelets exhibiting complex waveforms, often characterized by multiple voltage peaks. Evoked MGF membrane potential changes were detected in 93% of all stimuli delivered to anterior segment sensory fields, where head withdrawals are activated (n=11 preparations; Figure 5e). In contrast, stimulation of the body wall in posterior segments, within the LGF sensory field for tail withdrawal, never evoked membrane potential changes in the MGF (n=4 preparations; Figure 5f). Interestingly, stimulation of an anterior segment, while recording from the MGF axon of an adjacent segment, produced only EPSPs and large action potentials, but no spikelets were recorded (Figure 5g). This observation suggests that spikelets are only effectively generated in the segment of origin, and are not propagated between MGF axonal segments.

The three evoked MGF electrophysiological events, action potentials (APs), spikelets and EPSPs, were analyzed for amplitude and rate of voltage changes. Both APs and spikelets have rapid rising phases, whereas EPSPs have a slow onset and more sustained membrane depolarization (n=16; Figure 5h). Comparison of electrophysiological characteristics demonstrated that spikelets have a faster rise time (0.6±0.1 vs. 5.6±0.4 ms; $p<0.001$) and higher amplitude (12.1±0.9 vs. 6.1±0.5 mV; $p<0.001$) than did EPSPs recorded in the same MGFs (Figure 5i). In contrast, spikelets were much slower (dV/dt; 25.9±2.5 vs. 89.5±4.6 mV/ms; $p<0.001$) and smaller in amplitude than APs (63.8±3.3 mV; $p<0.001$; Figure 5j), suggesting that these events represent distinct, non-overlapping populations of evoked membrane potential changes. The unique electrophysiological characteristics of spikelets indicate they are likely generated by electrically coupled inputs to MGF.

Glutamatergic sensory activation of the MGF coupled network

Touch- and pressure-sensitive neural pathways are mediated by glutamatergic sensory inputs onto interneuronal targets in some annelids (Baccus et al., 2000; Burrell and Sahley, 2004; Grey and Burrell, 2010; Li and Burrell, 2011). To determine if glutamate mediates sensory afferent activation of the MGF pathway in *Lumbriculus*, glutamate receptor antagonists were applied to the issected preparations and exposed VNC. MGF responses to body wall stimulation were accessed. Electrophysiological recordings were performed following a 5 min treatment with 25μM CNQX (an AMPA/kainate receptor antagonist), 100μM AP5 (a NMDA receptor

antagonist) or physiological saline control (Figure 6a). No MGF EPSPs, spikelets or APs were detected in response to stimulation following application of CNQX (Figure 6b), although the full range of MGF spiking events were evoked following a saline bath application or a saline wash for 5 minutes subsequent to CNQX exposure. In contrast, AP5 had no effect on MGF evoked potentials, with EPSPs, spikelets and APs all persisting in its presence (Figure 6b). Note that due to the short duration of MGF penetrations, pharmacological treatments were not sequential, but conducted with separate giant axon penetrations (see Methods).

Analysis of excitatory postsynaptic potentials (EPSPs) demonstrated that CNQX treatment virtually abolished EPSPs, reducing the mean amplitude from 8.2±1.1 (n=11) to 0.5±0.2 mV (n=11; $p<0.01$; Figure 6c-d). In contrast, the suppression produced by AP5 treatment on EPSP amplitude was less than that of CNQX (5.0±0.4 mV; n=7) and was not significantly different from preparations following saline washout (5.0±1.3 mV, p=0.0645; n=5; Figure 6c-d). CNQX treatment also reduced the amplitude of miniature postsynaptic potentials (mPSPs) as compared to saline controls, where mPSP amplitudes were 1.9±0.2 mV (n=4) and 0.8±0.3 mV (n=11; p=0.0174) in control and treated preparations, respectively (Figure 6e-f). The amplitude of spontaneous mPSPs in CNQX was significantly different from washout values ($p<0.01$, n=5; Fig. ure 6e-f). Again, AP5 had no effect on mPSP amplitude (2.2±0.2 mV; n=7; p=0.3429; Figure 6e-f). The abolition of evoked MGF potentials by CNQX suggests that sensory-to-interneuronal synapses are exclusively glutamatergic.

Glutamate receptor immunoreactivity of the MGF coupled network

Since our ultrastructural studies revealed evidence for chemical synapses at both MGF collaterals and IGF bundles, we conducted glutamate receptor immunocytochemical staining on VNC cryosections and assessed glutamate receptor (GluR) antibody reactivity at these sites. Three ionotropic GluR antibodies known to cross-react with annelid (leech) nervous system (Thorogood et al., 1999) were used as potential synaptic markers, since MGF activation was abolished by CNQX, a glutamate receptor antagonist. Staining with an antibody to GluR5-7, which specifically recognizes subunits 5, 6, and 7 of kainate receptors in vertebrates, resulted in extensive immunoreactivity within the *Lumbriculus* VNC (Figure 7a; n=25). Much weaker immunoreactivity within the neuropile of the VNC was observed with a GluR2-3 antibody, which recognizes subunits 2 and 3 of vertebrate AMPA receptors (Figure 7b; n=2). A NR1 antibody, which recognizes subunit 1 of NMDA receptors, did not immunoreact with the VNC (Figure 7c; n=4). GluR5-7 staining was present at longitudinal muscle fibers and in gut tissues (not shown), but was most obvious as punctate labeling within the neuropile of the VNC (Figure 7d). This GluR antibody staining was localized to periaxonal regions of the giant fibers, including the dorsal MGF and LGFs (Figure 7e-f), the ventral giant fibers (VGFs; Figure 7g) and the IGF bundles (Figure 7h). Cross-sections of neurobiotin (NB)-filled MGF coupled networks revealed co-localized staining of GluR5-7 immunoreactivity and NB at periaxonal regions of the IGF bundles (Figure 7i-k), supporting glutamate receptor expression within the IGF bundles. GluR5-7 antibody staining was not obviously different between anterior and posterior segments

(data not shown), even though MGF activation by sensory stimulation was only detected in anterior segments. GluR antibody staining along the IGF processes, supports the idea that these sites of sensory input to the MGF, in anterior segments, are glutamatergic. Further, GluR antibody staining along posterior segments, in a region with no functional activity (Figure 5f), suggests the existence of non-functional (silent) glutamatergic synapses (Figure 8).

DISCUSSION

Two giant fiber pathways mediate rapid escape reflexes in most oligochaete worms, including *Lumbriculus*. The medial giant fiber (MGF) pathway, which triggers anterior body shortening, is activated by sensory inputs across the anterior 1/3 of the worm's body segments (Drewes, 1984; Zoran and Drewes, 1987). A variety of tactile and light stimuli activate lumbriculid GFs (Drewes, 1984; Smith and Mittenthal, 1980; Drewes and Fourtner, 1989). It was suggested many decades ago that MGF pathways are not principally activated by direct afferent inputs, but rather indirectly excited through smaller "giant" interneurons (Drewes, 1984). Here we demonstrate that the segmentally arranged medial giant axons are dye coupled to a network of such small interneurons, that we hypotheze serves as an electrically-coupled neural circuit for sensory processing.

Coupled MGF neural network

Electron microscopic studies, in earthworm and here in *Lumbriculus,* found no chemical synapses onto MGF collaterals (Drewes, 1984). For this reason, together with the constancy of PSP amplitude and the absence of failures during high frequency stimulation (Lybrand and Zoran, 2012), electrical synapses between these sensory interneurons and giant fibers are predicted to mediate afferent processing. Such a sensory system exists with respect to the S-cell

network of the leech. This through-conducting system along the leech ventral nerve cord receives sensory inputs from touch neurons via a pair of small interneurons that are electrically coupled to the S-cell (Muller and Scott, 1981). The low molecular weight dyes, Lucifer yellow and neurobiotin, but not the larger rhodamine dextran, passed readily across septal boundaries between adjacent segments of the *Lumbriculus* medial giant axon. In contrast, only neurobiotin diffused from the MGF into eight other interneurons and two the smaller, giant axons in each segment. MGF dye coupling with these two intermediate giant fibers (IGFs) was indicative of gap junctions and electrical synapses at IGF-MGF connections. Differences in dye permeability based on size are likely due to disparities in specific innexin protein expression among network neurons. In the medicinal leech, over 20 innexin genes are encoded in the genome and differential expression of innexins in central neurons underlies selective circuit connectivity (Kanadarian et al., 2012; Firme et al., 2012). In fact, disparate expression of innexins in identified annelid neurons alters neurobiotin coupling (Yazdani et al., 2013). Therefore, gap junction expression by interneuronal elements of a coupled network may underlie fundamentally different roles of specific connections during sensory processing.

Invertebrates myelin-like sheaths, including those of many annelids, are similar in function to those of vertebrates and annelid sheathes possess periodic gaps for current flow. These unmyelinated collaterals project into the cord neuropile of the VNC (Drewes, 1984; Zoran et al., 1988). Each of the four MGF collaterals per segment in *Lumbriculus* link to commissural crossbridges extending from the bilateral IGFs. Bilateral synchrony of GF spiking is mediated by

similar decussations of giant fiber neurites in numerous annelid worms, and cross talk between paired GFs in a polychaete worm, *Sabella,* results from direct electrical coupling at their commissural junctions (Mellon et al., 1980). Often these commissures are located close to the sites of GF spike initiation (Bullock, 1953; Hagiwara et al., 1964; Krasne, 1965). Whole mount dye-fill reconstructions and serial transmission electron microscopy of the *Lumbriculus* ventral cord identified the only feasible IGF-MGF contact sites as close appositions between IGF commissural crossbridges and MGF collaterals. Earthworm giant fiber collaterals are the putative sites of electrical synapses (Drewes, 1984) and, in the sludge worm, *Branchiura*, collateral dendrites are the sites of sodium channel localization and action potential generation (Zoran et al., 1988). Therefore, we suggest that a coupled IGF-MGF network constitutes an afferent processing conduit for the sensory activation of MGF-mediated escape.

Giant fibers of earthworms are activated by diverse mechanosensory modalities and the sensory systems that detect them evoke complex depolarizing PSPs of variable latency, amplitude and waveform in the GFs (Drewes, 1984). Stimulation of the body wall of *Lumbriculus* evoked three distinct electrophysiological responses in the MGF: (1) slow, long-duration graded PSPs, (2) fast, large amplitude APs of short duration and (3) fast, low amplitude spikelets of short duration (Figure 5h-j). Similar fast spikelets of small amplitude occur between rodent hippocampal neurons, where they strongly contributed to spiking activity as fast prepotentials (Epsztein et al., 2010). In fact, spikelets drive ~30% of all CA1 pyramidal cell action potentials during spatial exploratory behavior. Although the source of MGF spikelets

remains unknown, several possibilities are likely. First, spikelets may originate from the coupled IGF interneurons, since these cells are dye-coupled to the MGF. In crayfish, tail-flip escape behavior is activated by mechanosensory afferents connect via cholinergic synapses to secondary sensory interneurons that, in turn, are electrically coupled to the lateral giant (LG) interneurons that trigger the escape reflex (Zucker, 1972; Edwards et al., 1999). Excitation of the secondary interneuron brings the LG closer to threshold, thus priming the pathway for activation (Liu and Herberholz, 2010). Second, spikelets might originate in the MGF itself at electrotonically distant active sites, although this is less likely as spiklets are not activated by stimulation of neighboring body segments. If the intermediate giant interneurons are the source of spikelets, then they may function similarly to crayfish sensory interneurons in priming GF excitability. Although these IGF-MGF circuit components have been identified anatomically and physiologically, direct coupling between the two giant interneuronal pathways has not, and cannot, be measured. Therefore, we assume that IGF inputs can influence MGF activation, but cannot exclude the possibility that action potentials in the MGF drive current into the IGFs and activates them.

Sensory processing

Electrical synapses are ubiquitous in interneuron networks (Rela and Szczupak, 2004) and a common feature of escape neural circuits. Gap junctions allow for decreased synaptic delay, as compared to chemical synapses, and enhance network and behavioral speed. Additionally, electrically coupled neurons efficiently detect the coincidence of simultaneous, and

often subthreshold, depolarizing inputs (Amsalem et al., 2016; Galarreta and Hestrin, 1999; Pereda, 2014), influencing the excitability of coupled networks (van Welie et al., 2016; Alcami, 2018). The IGFs of *Lumbriculus* synchronously activate MGF collateral dendrites via electrical inputs, as indicated by spikelets recordings. These small diameter interneurons likely have a large input resistance and reach threshold for activation quickly. With the long space constant (approximately 3-6 mm) of annelid giant axons (Dierolf and Brink, 1973), the electrically coupled sensory interneurons may serve not only as a coincidence detector, but as a distributor of inputs among many neighboring MGF collaterals. Although the space constant is long, it is not sufficient to allow electronic spread of subthreshold spikelets along the intersegmental giant fiber pathways. Thus, spikelets are only detected in the MGF of a stimulated segment. In earthworms, spatial summation of sensory inputs encompasses as many as 5 body segments (Drewes, 1984), and in *Lumbriculus* this would equate to over 20 collateral dendrites. When coincident electrical synaptic currents impinge on coupled cells, like the segmentally-arranged giant axons of *Lumbriculus*, the excitability of the coupled neurons is increased and the coincident inputs are more efficiently integrated (Di Garbo et al., 2007; Hjorth et al., 2009). For example, the probability and latency of stimulus-triggered action potentials among cerebellar basket cells are increased upon simultaneous excitation of their electrical synapses (Alcami, 2018). We propose that the spikelets recorded in the MGF following body wall stimulation are the neurophysiological signatures of IGF electrical inputs and whose coincident detection at MGF collaterals more efficiently drive giant axon activation.

Electrical synapses are also highly effective at enhancing the sensitivity of sensory systems, particularly of primary afferents of escape neural networks (Herberholz et al., 2002; Curti and Pereda, 2004). Synchronous sensory inputs reduce shunting of synaptic currents of GF dendrites, effectively increasing input resistance and making PSP amplitudes larger. Thus, simultaneous inputs across many MGF collaterals would experience little difference in membrane voltage and therefore less shunting of their synaptic currents. In the escape neural network of crayfish, interafferent coupling selectively amplifies converging inputs to the lateral giant axon (Antonsen and Edwards, 2003). Gap junction-coupled neural circuits in the nematode worm, *C. elegans*, modulate mechanosensory processing, such that active input neurons facilitate the network and inactive inputs suppress the network through shunting (Rabinowitch et al., 2013). Furthermore, electrical and chemical synapses, when expressed at shared sites of contact, can mutually regulate each other's formation and function (Jabeen and Thirumalai, 2018). Gap junctions between premotor interneurons and motor neurons can lead to amplified chemical transmission at mixed synapses and disrupting electrical synaptic function can inhibit chemical transmission (Liu et al., 2017). In the case of *Lumbriculus*, MGF excitability might be enhanced directly by the depolarizing current input of the electrically-coupled sensory interneuron and be important at coincident multisegmental inputs converging upon collateral sites, as compared to unisegmental inputs.

Adaptive significance of the coupled MGF network

A mechanosensory network, similar to that observed here, exists in the nematode worm, *C. elegans*, where converging inputs and coincidence detection are the basis for distinct responses to distributed and localized inputs (Rabinowitch et al., 2013). Such a hub-and-spoke motif circuitry for the coincident detection of sensory inputs described for the nematode seems quite reasonable as a model for the role of MGF collaterals during escape behavior in lumbriculid worms. Our dye tracings, serial reconstructions, ultrastructural analyses, electrophysiological recordings and immunostaining combine to suggest that the collateral dendrites of the MGF, in fact, function as central gatekeepers of interneuronal input to the spike initiation centers of these command interneurons. The commonalities of synchronous inputs, summation and facilitation of synaptic potentials and coincidence detection at hub-and-spoke convergences within sensory circuits across a wide range of animal species suggests that they have evolved not only as characteristic features of escape neural circuits, but for sensory processing networks in general across animal taxa.

CONFLICT OF INTEREST

The authors declare that they have no conflict of interest.

AUTHOR CONTRIBUTIONS

Z.R.L., V.G.M-A., and M.J.Z. designed and performed, Z.R.L. and M.J.Z. analyzed data; and Z.R.L., V.G.M-A., and M.J.Z. wrote the paper.

ORCID

Zane Lybrand https://orcid.org/0000-0003-1543-8155

Veronica Martinez-Acosta https://orcid.org/0000-0003-3402-0379

Mark Zoran https://orcid.org/00000-0001-8137-7480

REFERENCES

Alcami P. (2018). Electrical synapses enhance and accelerate interneuron recruitment in response to coincident and sequential excitation. *Front Cell Neurosci* 12, 156.

Amsalem O, Van Geit W, Muller E, Markram H, and Segev I. (2016). From neuron biophysics to orientation selectivity in electrically coupled networks of neocortical L2/3 large basket cells. *Cereb Cortex* 26, 3655-3668.

Antonsen BL, Edwards DH. (2003). Differential dye coupling reveals lateral giant escape circuit in crayfish. *J Comp Neurol* 466(1), 1-13.

Baccus SA, Burrell BD, Sahley CL, Muller KJ. (2000). Action potential reflection and failure at axon branch points cause stepwise changes in EPSPs in a neuron essential for learning. *J Neurophysiol* 83(3), 1693-1700.

Bullock TH. (1953). Properties of some natural and quasi-artificial synapses in polychaetes. *J Comp Neurol* 98, 37-68.

Burrell BD, Sahley CL. (2004). Multiple forms of long-term potentiation and long-term depression converge on a single interneuron in the leech CNS. *J Neurosci* 24(16), 4011-4019.

Curti S, Pereda AE. (2004). Voltage-dependent enhancement of electrical coupling by a subthreshold sodium current. *J Neurosci* 24, 3999-4010.

Dierolf BM, Brink PR. (1973). Effects of temperature acclimation on cable constants of the earthworm median giant axon. *Comp Biochem Physiol* 44, 401-406.

Drewes C, D. (1984). Escape reflexes in earthworms and other annelids. In: Eaton RC, editor. *Neural mechanisms of startle behavior*. Plenum Press. pp. 43-91.

Drewes CD, Fourtner CR. (1989). Hindsight and rapid escape in a freshwater oligochaete. *Biol Bull* 177, 363-371

Drewes CD, Fourtner CR. (1990). Morphallaxis in an aquatic oligochaete, *Lumbriculus variegatus*: reorganization of escape reflexes in regenerating body fragments. *Dev Biol* 138(1), 94-103.

Edwards DH, Heitler WJ, Krasne FB. (1999). Fifty years of a command neuron: the neurobiology of escape behavior in the crayfish. *Trends Neurosci* 22(4), 153-161.

Epsztein J, Lee AK, Chorev E, Brecht M. (2010). Impact of spikelets on hippocampal CA1 pyramidal cell activity during spatial exploration. *Science* 327, 474-477.

Firme CP, Natan RG, Yazdani N, Macagno ER, Baker MW. (2012). Ectopic expression of select innexins in individual central neurons couples them to pre-existing neuronal or glial networks that express the same innexin. *J Neurosci* 32(41), 14265-70.

Galarreta M, Hestrin S. (1999). A network of fast-spiking cells in the neocortex connected by electrical synapses. *Nature* 402, 72–75.

Grey KB, Burrell BD. (2010). Co-induction of LTP and LTD and its regulation by protein kinases and phosphatases. *J Neurophysiol* 103(5), 2737-2746.

Grey KB, Moss BL, Burrell BD. (2009). Molecular identification and expression of the NMDA receptor NR1 subunit in the leech. Invert Neurosci 9(1), 11-20.

Gunther J. (1975). Neuronal syncytia in the giant fibres of earthworms. *J Neurocytol* 4(1), 55-62.
Hagiwara S, Morita H, Naka K. (1964). Transmission through distributed synapses between two giant axons of a sabellid worm. *Comp Biochem Physiol* 13, 453-460.
Hartline DK, Colman DR. (2007). Rapid conduction and the evolution of giant axons and myelinated fibers. *Curr Biol* 17(1), R29-35.
Herberholz J, Antonsen BL, Edwards DH. (2002). A lateral excitatory network in the escape circuit of crayfish. *J Neurosci* 22, 9078-9085.
Herberholz J, Marquart GD. (2012). Decision making and behavioral choice during predator prey avoidance. *Front Neurosci* 6, 125.
Huntley GW, Rogers SW, Moran T, Janssen W, Archin N, Vickers JC, Cauley K, Heinemann SF, Morrison JH. (1993). Selective distribution of kainate receptor subunit immunoreactivity in monkey neocortex revealed by a monoclonal antibody that recognizes glutamate receptor subunits GluR5/6/7. *J Neurosci* 13(7), 2965-2981.
Jabeen S, Thirumalai V. (2018). The interplay between electrical and chemical synaptogenesis. *J Neurophysiol* 120, 1914-1922.
Jamieson BGM. (1981). *The ultrastructure of the oligochaete.* Academic Press.
Kandarian B, Sethi J, Wu A, Baker M, Yazdani N, Kym E, Sanchez A, Edsall L, Gaasterland T, Macagno E. (2012). The medicinal leech genome encodes 21 innexin genes: different combinations are expressed by identified central neurons. *Dev Genes Evol* 222(1), 29-44.
Kensler RW, Brink PR, Dewey MM. (1979). The septum of the lateral axon of the earthworm: a thin section and freeze-fracture study. *J Neurocytol* 8(5), 565-590.
Krasne FB. (1965). Escape from recurring tactile stimulation in *Branchiomma vesiculosum*. *J Exp Biol* 42, 307-322.
Krasne FB, Teshiba TM. (1995). Habituation of an invertebrate escape reflex due to modulation by higher centers rather than local events. *Proc Natl Acad Sci* USA 92, 3362-3366.
Li Q, Burrell BD. (2011). Associative, bidirectional changes in neural signaling utilizing NMDA receptor- and endocannabinoid-dependent mechanisms. *Learn Mem* 18(9), 545-553.
Liu P, Chen B, Mailler R, Wang Z-W. (2017). Antidromic-rectifying gap junctions amplify chemical transmission at functionally mixed electrical-chemical synapses. *Nature Communications* 8, 14818.
Liu Y-C, Herberholz J. (2010). Sensory activation and receptive field organization of the lateral giant escape neurons in crayfish. *J Neurophysiol* 104, 675-684.
Lybrand ZR, Zoran MJ. (2012). Rapid neural circuit switching mediated by synaptic plasticity during morphallactic regeneration. *Dev Neurobiol* 72, 1256-1266.
Malenka RC, Nicoll RA. (1997). Silent synapses speak up. *Neuron* 19, 473-476.
Martinez VG, Menger GJ, 3rd, Zoran MJ. (2005). Regeneration and asexual reproduction share common molecular changes: upregulation of a neural glycoepitope during morphallaxis in *Lumbriculus*. *Mech Dev* 122(5),721-732.

Mellon D, Treherne JE, Lane NJ, Harrison JB, Langley CK. (1980). Electrical interactions between the giant axons of a polychaete worm (*Sabella penicillus* L.). *J Exp Biol* 84,119-36.

Muller KJ, Scott SA. (1981). Transmission at a 'direct' electrical connexion mediated by an interneurone in the leech. *J Physiol* 311, 565-583.

Pereda AE, Rash JE, Nagy JI, Bennett MVL. (2004). Dynamics of electrical transmission at club endings on the Mauthner cells. *Brain Res Rev* 47, 227-244.

Pereda AE. (2014). Electrical synapses and their functional interactions with chemical synapses. *Nat Rev Neurosci* 15(4), 250-63.

Petralia RS, Wenthold RJ. (1992). Light and electron immunocytochemical localization of AMPA-selective glutamate receptors in the rat brain. *J Comp Neurol* 318(3), 329-354.

Petralia RS, Yokotani N, Wenthold RJ. (1994). Light and electron microscope distribution of the NMDA receptor subunit NMDAR1 in the rat nervous system using a selective anti-peptide antibody. *J Neurosci* 14(2), 667-696.

Rabinowitch I, Chatzigeorgiou M, Schafer WR. (2013). A gap junction circuit enhances processing of coincident mechanosensory inputs. *Curr Biol* 23(11), 963-967.

Rela L, Szczupak L. (2004). Gap junctions: their importance for the dynamics of neural circuits. Mol Neurobiol 30, 341–357.

Schweigreiter R, Roots BI, Bandtlow CE, Gould RM. (2006). Understanding myelination through studying its evolution. *Int Rev Neurobiol* 73:219-273.

Siegel SJ, Janssen WG, Tullai JW, Rogers SW, Moran T, Heinemann SF, Morrison JH. (1995). Distribution of the excitatory amino acid receptor subunits GluR2(4) in monkey hippocampus and colocalization with subunits GluR5-7 and NMDAR1. *J Neurosci* 15(4), 2707-2719.

Smith PH, Mittenthal JE. (1980). Intersegmental variation of afferent pathways to giant interneurons of the earthworm *Lumbricus terrestris*. *Journal of Comparative Physiology A: Neuroethology, Sensory, Neural, and Behavioral Physiology* 140(4), 351-363.

Thorogood MS, Almeida VW, Brodfuehrer PD. (1999). Glutamate receptor 5/6/7-like and glutamate transporter-1-like immunoreactivity in the leech central nervous system. *J Comp Neurol* 405(3), 334-344.

van Welie I, Roth A, Ho SS, Komai S, Häusser M. (2016). Conditional spike transmission mediated by electrical coupling ensures millisecond precision-correlated activity among interneurons in vivo. *Neuron* 90, 810-823.

Yazdani N, Firme CP, Macagno ER, Baker MW. (2013). Expression of a dominant negative mutant innexin in identified neurons and glial cells reveals selective interactions among gap junctional proteins. *Dev Neurobiol* 73(8), 571-86.

Zoran MJ, Drewes CD. (1987). Rapid escape reflexes in aquatic oligochaetes: variations in design and function of evolutionarily conserved giant fiber systems. *Journal of Comparative Physiology A: Neuroethology, Sensory, Neural, and Behavioral Physiology* 161(5), 729-738.

Zoran MJ, Drewes CD, Fourtner CR, Siegel AJ. (1988). The lateral giant fibers of the tubificid worm, Branchiura sowerbyi: structural and functional asymmetry in a paired interneuronal system. *J Comp Neurol* 275(1), 76-86.

Zoran MJ, Martinez VG. (2009). *Lumbriculus variegatus* and the Need for Speed: A Model System for Rapid Escape, Regeneration and Asexual Reproduction, in Annelids in Modern Biology. In: Shain DH, editor. *Annelids in Modern Biology*. Hoboken, NJ: John Wiley & Sons, Inc.

Zucker RS. (1972). Crayfish escape behavior and central synapses. I. Neural circuit exciting lateral giant fiber. *J Neurophysiol* 35(5), 599-620.

TABLES

Table 1.

List of Primary Antibodies

Monoclonal Antibody	Immunogen/Host	Source
Anti-GluR5,6,7 (1:50 dilution)	TrpE-GluR5 (aa: 233-518)/mouse (recombinant fusion protein)	(Abcam Cat# ab77739, RRID:AB_1566261)
Anti-GluR2,3 (1:33 dilution)	Rabbit Ser880/891 of GluR2+3/mouse (synthetic peptide)	(Abcam Cat# ab52896, RRID:AB_880229)
Anti-NMDAR1 (NR1) (1:33 dilution)	Rat NMDAR1 (aa:660-811)/mouse (recombinant protein)	(BD Biosciences Cat# 556308, RRID:AB_396353

Table 2.

List of Secondary Antibodies

Secondary Antibody	Working dilution	Source
Goat anti-mouse IgG_1(γ1) Alexa Fluor 555	1:1000	(Molecular Probes Cat# A-21127, RRID:AB_141596)
Goat anti-mouse IgM (μ) Alexa Flour 555	1:1000	(Innovative Research Cat# A21426, RRID:AB_1500929)
Goat anti-mouse IgM (μ) Alexa Flour 488	1:1000	(Molecular Probes Cat# A-21042, RRID:AB_141357)

FIGURE LEGENDS

Figure 1. The MGF coupled network and its longitudinal organization. (a) The fluorescent dye, Lucifer yellow, spread both anteriorly and posteriorly along the medial giant fiber (MGF) when injected into the axon. A single medial giant soma (MS) accumulated the fluorescent dye in each body segment at the level of the bilateral pairs of setae (Se), which are autofluorescent and positioned within the body wall adjacent to the ventral nerve cord (VNC). Lucifer yellow readily diffused across septal boundaries (SB), which are the sites of gap junctional coupling between neighboring segmentally-arranged axons of the MGF. Lucifer yellow also accumulated in multiple giant fiber collaterals (MC) in each segment. Injected anterior preparations; n=6. (b) The neurotracer dye, neurobiotin (NB), was injected into a medial giant axon (out of the plane of focus in this image) of an anterior body segment. NB dye diffused along the medial giant fiber as well as into several other neurons and processes within anterior segments of the ventral nerve cord (n=20 preparations). Besides the MS, eight other neuronal somata became visible following NB injection and staining. Four dye-coupled somata were positioned laterally within the cord (arrowheads) and four cell bodies were located in the medial cord (arrows). (c) NB-injected medial giant fibers (MGF) were dye-coupled to smaller diameter intermediate giant fibers (IGF) and their paired cell bodies (arrows). The IGF extended parallel to the MGF along the nerve cord. (d) An illustration of the MGF/IGF coupled system (longitudinal perspective) summarizes the dye-coupled elements of the network for anterior escape in one segment relative to two VNC landmarks: the segmentally-arranged setae and the segmental nerves. This illustration indicates

that dye tracing was restricted to the ventral nerve cord, with no dye-filled processes extending into peripheral body wall tissues. Each body segment contained nine dye-coupled cell bodies, including one medial giant interneuron (MS) and two intermediate giant interneurons (I) and 6 are unidentified interneurons. Four medial giant axon collaterals (white clusters; MC), four intermediate giant axon cross-bridges and one medial giant interneuron septal boundary (chevron; SB) were also stereotypically arranged within each segment of VNC. Note that in all panels the VNC is oriented with anterior is to left and posterior is to the right. Scale bars in (a) equals 30 μm. Scale bars in (b) and (c) equal 20 μm.

Figure 2. The MGF/IGR coupled network and its cross-sectional organization. (a) Lucifer yellow dye accumulated in ventrally projecting medial giant fiber collateral (MC), the soma (MS) and to a lesser degree at septal boundaries between coupled axons (SB). (b) Neurobiotin tracer revealed regularly spaced cross-bridges (CB) connecting the paired medial intermediate giant fibers. The CBs were typically located in close proximity to the dye filled IGF somata (IS), which were linked to the fibers by fine dye-filled processes (arrow). (c) Cross-section of the VNC in anterior segments of neurobiotin-injected MGFs revealed two distinct small diameter IGFs within the neuropile ventral to larger MGF. The neurobiotin labeled medial giant interneuron soma (MS) and the intermediate giant interneuron soma (IS) were located ventromedially and laterally in the VNC, respectively. Fine processes filled with dye connected the IS to the IGF (arrow). (d) An illustration of the MGF/IGF coupled system (cross-sectional

perspective) summarizes the dye-coupled elements of the network for anterior escape at the level of an MGF collateral. The MGF collateral (white spheres) are located in close proximity to the IGF crossbridges. These potentials sites of MGF-IGF contact often occur in sections containing both MGF and IGF interneuronal somata (MS and IS). Scale bars in (a) and (b) equal 15 µm. Note that in panels (a) and (b) the VNC is oriented with anterior is to left and posterior is to the right. In panels (c) and (d), the dorsal aspect of the VNC is at the top. Scale bars in (c) equals 20 µm.

Figure 3. Ultrastructure of MGF and IGF axons. (a) Cross-section of the MGF from an anterior body segment with a collateral (Co) protruding ventrally through an opening in the loose myelin-like sheath (MyS). (b) High magnification image of a collateral region (MGF Co) containing numerous densely clustered synaptic vesicles adjacent to thickened neuron membranes (arrows). (c) Cross-section through an IGF bundle showing 4-5 small diameter axons of intermediate giant interneurons. (d) Translucent and dense-core synaptic vesicle clusters where associated with IGF interneuronal bundles at sites of thickened neuronal membranes (arrows).

Figure 4**.** Ultrastructure of MGF-IGF contacts. (a) Cross-section through the ventral nerve cord (VNC) of a posterior body segment shows the three myelinated dorsal giant axons: a medial giant fiber (M) flanked by two lateral giant fibers (L). The MGF collateral (MC) extends ventrally into the neuropile of the VNC. Intermediate giant fiber crossbridges, indicated by

asterisks (*), are located ventrolaterally to the MGF collateral. (b) Higher magnification of MGF collateral cluster (MC) regions (white box) illustrates an IGF cross-bridge (CB) that extends from the IGF bundle to the MGF collateral. (c) Higher magnification of MGF collateral boxed area in panel (b) shows a site of collateral-crossbridge apposition (arrow). In all panels, the dorsal aspect of the VNC is at the top.

Figure 5. MGF evoked excitation involves small amplitude spikelets. (a) Dissected preparation illustrating a Lucifer-filled MGF the site of interacellular microelectrode recording and segmental sites of body wall simulation. Suction electrodes were placed adjacent to segmental nerves (SN) for sensory pathways activation of MGF excitation. (b) Body wall activation evoked multiple electrophysiological events in medial giant axons, including subthreshold excitatory postsynaptic potentials (EPSP). (c) Spikelets (Sp) were commonly elicited by sensory input activation. (d) Large MGF action potentials and spikelets were both activated by body wall stimulation. (e-f) Body wall stimulation evoked MGF electrophysiological events (APs, spikelets and EPSPs) in anterior segments (e), but not in posterior segments (f). G) Stimulation of body wall in an adjacent anterior segment (* in panel a), while recording from the MGF axon of the neighboring segment, produced only EPSPs and large action potentials, but no spikelets. (h) Superimposed MGF electrophysiology events illustrate differences in amplitude and timing characteristics of action potentials (magenta), spikelets (green) and EPSPs (blue). (i) Comparison of spikelets (green circles) and EPSPs (blue circles) demonstrate differences in rise time and

amplitude. (j) Comparison of spikelets (green circles) and action potentials (magenta circles) demonstrate differences in rate of voltage change and amplitude. Spikelet characteristics indicate they are distinct evoked events from APs and EPSPs. Vertical bar equals 10 mV and horizontal bar equals 5 ms in (b-g).

Figure 6. Glutamate antagonism of MGF pathway activation. (a) Dissected preparations were treated for 5 minutes prior to penetration of the MGF with an intracellular microelectrode and during one minute of electrophysiological recording. Preparations treated with pharmacological agents were then washed with saline for 5 minutes before a one-minute recording to assess recovery of function following drug washout. (b) Examples of saline control, CNQX, AP5 and saline wash recording are shown. Brief electrical stimulation of the body wall (lower traces) elicited EPSPs that generated action potentials or spikelets in saline and AP5 conditions. Treatment with CNQX abolished stimulus-evoked MGF activation. (c) Evoked PSPs were abolished by CNQX, but not AP5 treatment. Preparations treated with the antagonist for 5 minutes and subsequently washed for 5 minutes with saline possessed PSP amplitudes that were greater than those in CNQX. (d) Quantification of evoked PSP amplitudes demonstrated significant reductions following CNQX treatment as compared to control and washout preparations. a: saline-CNQX ($p<0.01$), b: saline-AP5 ($p<0.01$), c: saline-washout ($p<0.05$), d: CNQX-AP5 ($p<0.01$), e: CNQX-washout ($p<0.01$). (e) Representative traces of spontaneous PSPs recorded in presence of glutamate receptor antagonists or saline. (f) Quantification of

spontaneous PSP amplitudes demonstrated significant reductions following CNQX treatment as compared to control and washout preparations. f: saline-CNQX ($p<0.01$), g: CNQX-washout ($p<0.01$). Error bars presented as standard deviation. Saline, n=4; CNQX, n=11; AP5, n=7; Washout, n=5. Scale bars equal (b) 10 mV (vertical) and 5 ms (horizontal); (c) 2 mV (vertical) and 2 ms (horizontal) and (e) 1 mV (vertical) and 0.1 ms (horizontal).

Figure 7. Glutamate receptor immunoreactivity. (a) Cross-section of the VNC from anterior body segments was densely labeled with a GluR5-7 monoclonal antibody, particularly in with the neuropile. (b) GluR2-3 immunoreactivity was weak in the VNC neuropile, although staining outside the VNC was present. (c) VNC from anterior body segments was not labeled with a NR1 monoclonal antibody. Scale bar equals 50 μm in a-c. (d) GluR5-7 immunoreactivity was localized to periaxonal regions of the giant interneurons, indicated by boxes. (e-h) Higher magnification of the boxed areas in (d) show images of GluR5-7 immunoreactivity and illustrate punctate GluR staining at regions adjacent to the MGF (e), LGF (f), VGF (g) and IGF (h) axons. Scale bar equals 5 μm in e-h. Sharpness and contrast has been adjusted for panel d-h to best visualize staining from background. (i-k) Neurobiotin tracing of IGFs in MGF dye-injected preparations colocalized with GluR antibody staining.

Figure 8. Functional glutamatergic sensory inputs onto the MGF coupled network. (a) Schematic of the medial giant fiber (MGF) coupled network in anterior and posterior segments are

composed of a sensory neuron (dark blue spheres), the paired intermediate giant fibers and crossbridge (light green) and the medial giant fiber (magenta) with collaterals (white spheres). Glutamatergic synapses (indicated by blue ovals) are functional in anterior segments, but silent in posterior segments (green ovals). (b) Electrical signals recorded in MGFs of anterior segments following body wall stimulation include evoked postsynaptic potentials (EPSPs, blue), spikelets (green), and action potentials (magenta). None of these electrical signals are detected in posterior segments after sensory stimulation of the body wall. Although direct electrical coupling is not possible to assess in this preparation, we hypothesize that spikelets are derived from IGF spike currents spreading via collaterals to the MGF.

Figure 1

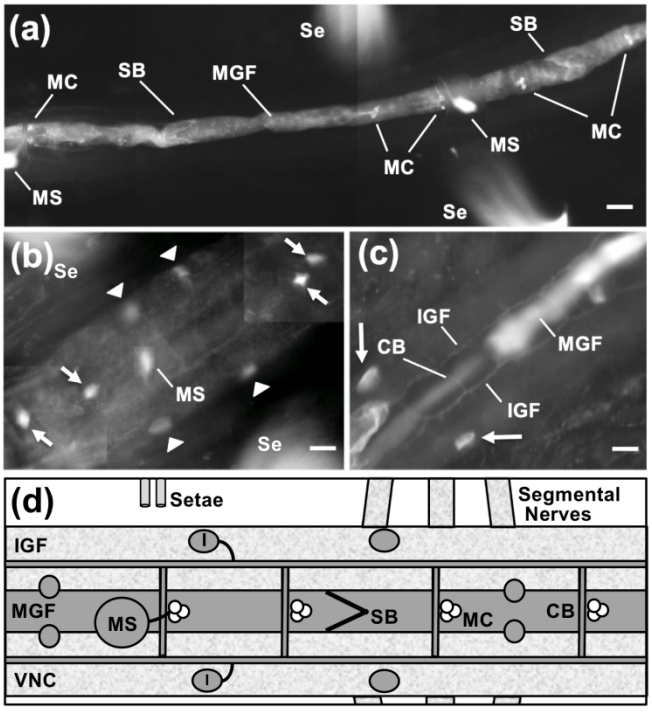

Figure 2

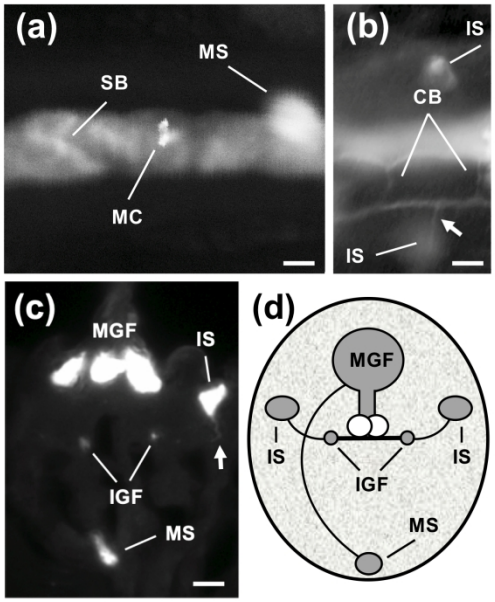

Figure 3

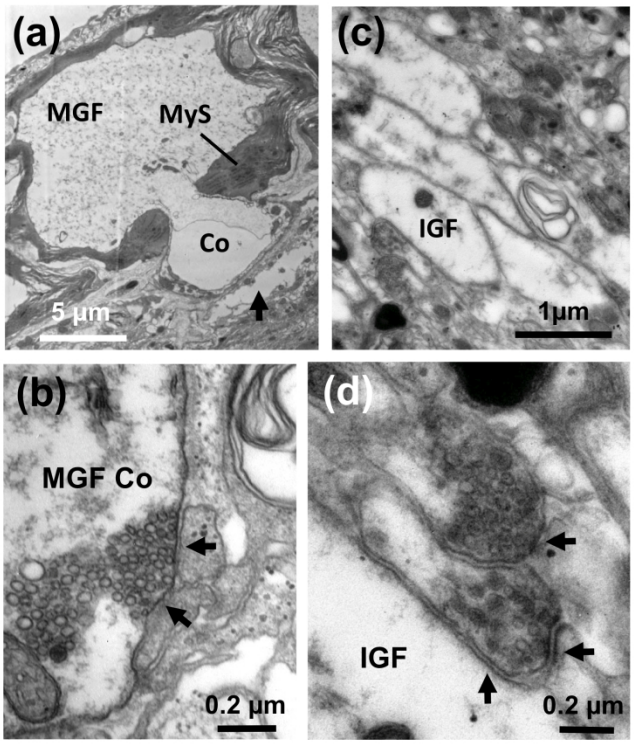

Figure 4

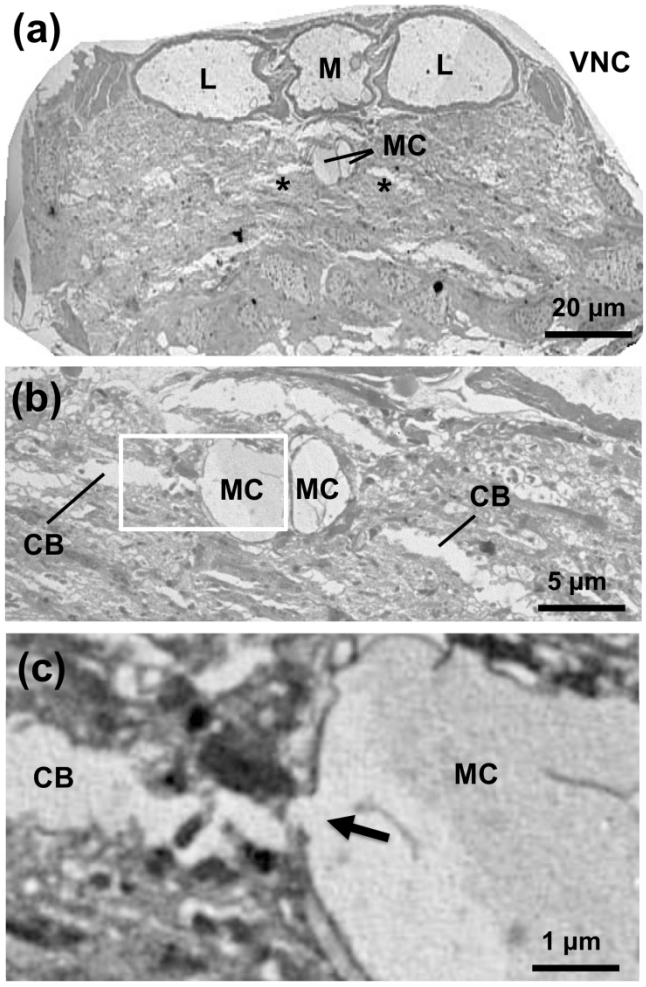

Figure 5

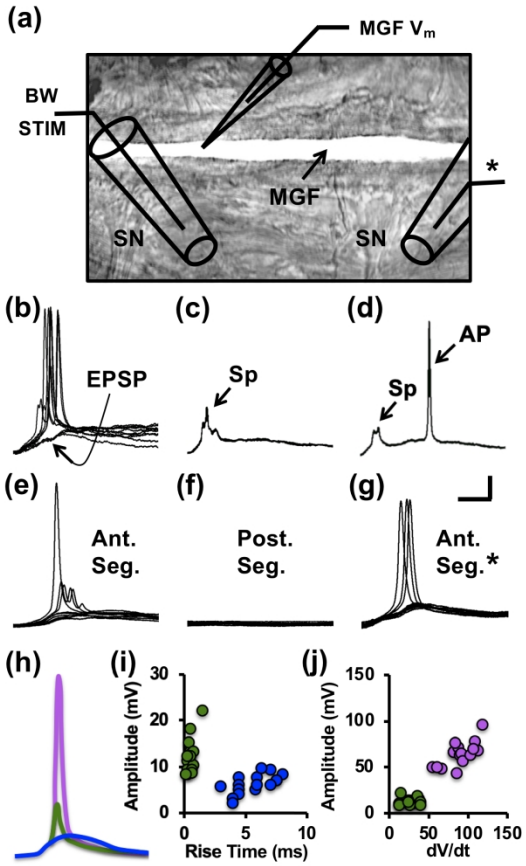

Figure 6

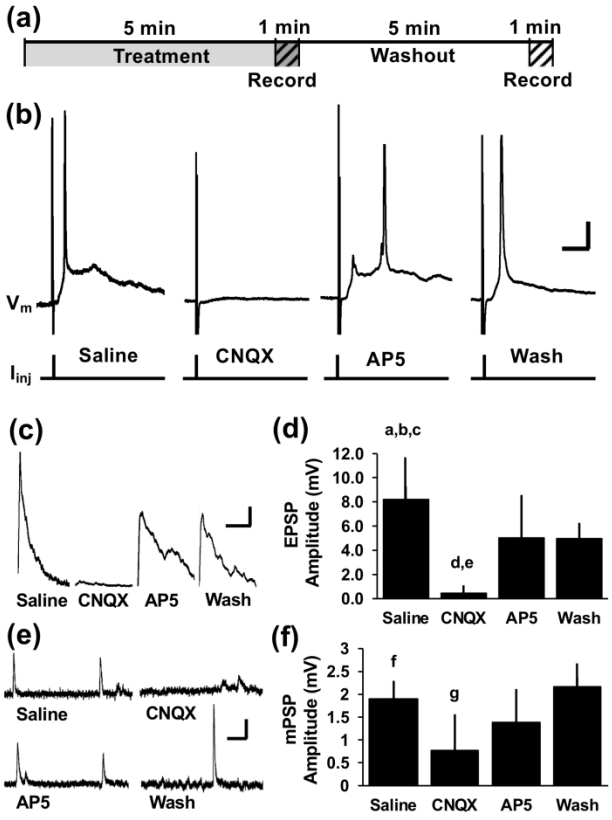

Figure 7

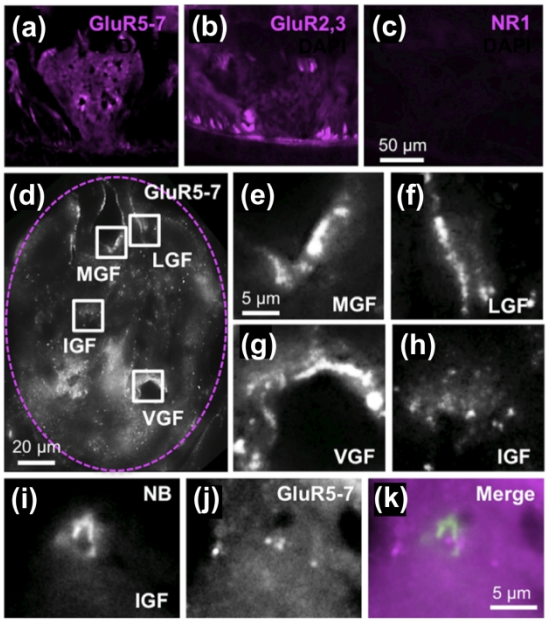

Figure 8

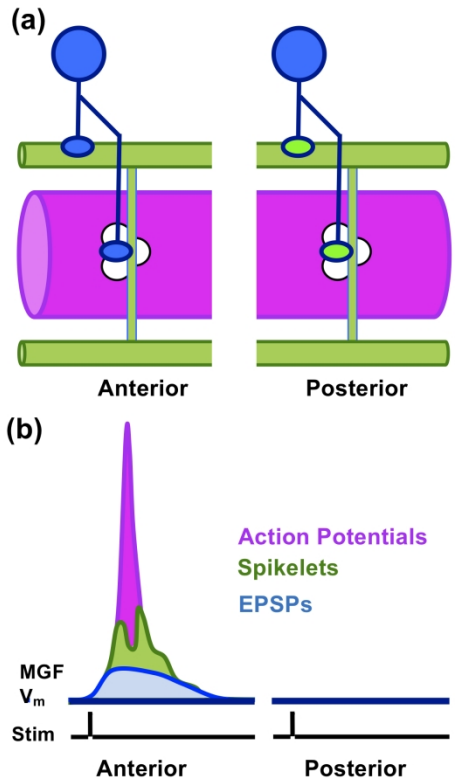

Table 1.

List of Primary Antibodies

Monoclonal Antibody	Immunogen/Host	Source
Anti-GluR5,6,7 (1:50 dilution)	TrpE-GluR5 (aa: 233-518)/mouse (recombinant fusion protein)	(Abcam Cat# ab77739, RRID:AB_1566261)
Anti-GluR2,3 (1:33 dilution)	Rabbit Ser880/891 of GluR2+3/mouse (synthetic peptide)	(Abcam Cat# ab52896, RRID:AB_880229)
Anti-NMDAR1 (NR1) (1:33 dilution)	Rat NMDAR1 (aa:660-811)/mouse (recombinant protein)	(BD Biosciences Cat# 556308, RRID:AB_39635

Table 2.

List of Secondary Antibodies

Secondary Antibody	Working dilution	Source
Goat anti-mouse IgG_1(γ1) Alexa Fluor 555	1:1000	(Molecular Probes Cat# A-21127, RRID:AB_141596)
Goat anti-mouse IgM (μ) Alexa Flour 555	1:1000	(Innovative Research Cat# A21426, RRID:AB_1500929)
Goat anti-mouse IgM (μ) Alexa Flour 488	1:1000	(Molecular Probes Cat# A-21042, RRID:AB_141357)

GRAPHICAL ABSTRACT

The giant interneuron (magenta) for rapid escape in the mud worm, *Lumbriculus variegatus*, is activated by sensory interneuron inputs (green) to its collateral dendrites. These sites of electrical coupling from sensory interneurons to the giant interneuron collaterals (blue) and generate spikelets in the giant interneuron (green recording), which we suggest sum with postsynaptic potentials (blue recording) and regulate sensory processing by priming giant axon spiking (magenta recording).